1960

A study of a 35 kilomegacycle cavity maser.

Reedy, Thomas M.

Monterey, California: U.S. Naval Postgraduate School

A STUDY OF A 35 KILOMEGACYCLE CAVITY MASER

THOMAS M. REEDY

UNITED STATES
NAVAL POSTGRADUATE SCHOOL

THESIS

A STUDY OF A 35 KILOMEGACYCLE CAVITY MASER

by

Thomas M. Reedy

Captain, U.S. Marine Corps

12ND P2238 (1-59)

A STUDY OF A 35 KILOMEGACYCLE CAVITY MASER

* * * * * *

Thomas M. Reedy

A STUDY OF A 35 KILOMEGACYCLE CAVITY MASER

by

Thomas M. Reedy

Captain, U. S. Marine Corps

Submitted in partial fulfillment of
the requirements for the degree of

MASTER OF SCIENCE
IN
ENGINEERING ELECTRONICS

United States Naval Postgraduate School
Monterey, California

1 9 6 0

A STUDY OF A 35 KILOMEGACYCLE CAVITY MASER

by

Thomas M. Reedy

This work is accepted as fulfilling

the thesis requirements for the degree of

MASTER OF SCIENCE

IN

ENGINEERING ELECTRONICS

from the

United States Naval Postgraduate School

ABSTRACT

A simplified classical theory of the three level cavity maser is presented. The significant characteristics of rutile (TiO_2) doped with Fe^{+++} are discussed with reference to its use in a maser. Thermal isolation problems and the microwave circuitry are examined. Experimental results for a cavity maser designed to amplify frequencies above 30 kmc/sec are discussed.

The author wishes to express his thanks to Professor Carl E. Menneken for his encouragement and also to Mr. Roy W. Roberts and Mr. Hal D. Tenney of Melabs for their excellent advice and help throughout the ten weeks at Melabs where the material for this paper was gathered.

TABLE OF CONTENTS

Title

LIST OF ILLUSTRATIONS

LIST OF SYMBOLS

A	area in cm^2
E_i	Energy of level i
f_{ij}	frequency of energy difference between levels i and j in cps
F	noise figure
g	gyromagnetic ratio
G	power gain
$g(f)$	line shape factor
h	Planck's constant = 6.625×10^{-27} erg-sec
$\hbar$	$h/2$
H_{ij}	Peak value of a linearly polarized RF magnetic field at the frequency of the transition between level i and j.
J	Quantum number dependent on orbital angular momentum of ion
k	Boltzmann's constant = 1.38×10^{-23} joules/°K
°K	degrees Kelvin = °C = 273+18
n_i	population of level i
N	total population or population per unit volume
N_i	thermal equilibrium population of level i
N_o	ambient noise power per cycle
P	power transferred in milliwatts
P_{abs}	power absorbed
P_n	effective noise power
R	inversion ratio
R_e	characteristic impedance of a transmission line
S	Quantum number denoting "effective" spin angular momentum

t	time
T	temperature in °Kelvin
T_e	effective input noise temperature
Te_{ij}	overall noise temperature of network i cascaded with network j
T_1	spin-lattice relaxation time
T_2	spin-spin relaxation time
w_{ij}	spontaneous transition probability between level i and j
W_{ij}	induced proability of a transition from level i to level j
W_{stored}	energy stored
β	Bohr magneton = .9274 X 10^{-20} erg/gauss
ΔH	line width between maximum slope points
$\Delta T/\Delta L$	temperature gradient °K/cm
$\rho^2(\psi_1\psi_2\psi_3)$	factor to account for non optimum orientation of the RF magnetic field
σ	thermal conductivity in mw/ cm-°K
μ_c	Magnetic moment
$\langle \mu_{ij} \rangle$	matrix element of the magnetic moment operator between states i and j normalized with respect to a S = 1/2 system
ω_{ij}	frequency of the transition between level i and j in radians/sec
η	filling factor = $\dfrac{\int_{crystal} \rho^2(\psi_1\psi_2\psi_3)\, H_{ij}^2\, dV}{\int_{cavity} H_{ij}^2\, dV}$

SECTION I

Introduction

A. Background

The CW solid state maser[1] amplifier was originally proposed in 1956 [1]. Since that time it has been developed into a device capable of certain system applications where a very low noise preamplifier is the dominating requirement. Successful masers have been operated in the laboratory from 300 mc/sec up to about 20 kmc/sec. The majority of these devices have used either potassium chromicyanide, $K_3\ Cr(CN)_6$, in potassium cobalticyanide, $K_3Co(CN)6$, or Cr^{+++} in ruby, Al_2O_3, as the active material. Neither of these materials is capable of amplification above approximately 20 kmc/sec without the use of excessively large magnetic fields.

The objective of this experiment was to extend the state of the art of maser development further into the microwave region by obtaining amplification in the vicinity of 35 kmc/sec. This was to be accomplished by using a rutile (TiO_2) crystal and a pumping frequency near 70 kmc/sec.

B. Possible applications

The applications listed below show a few of the areas where a microwave maser preamplifier could be employed usefully.

1. An acronym developed from "microwave amplification by stimulated emission of radiation". This paper is limited to consideration of only one type of maser - the CW solid state cavity maser. Other variations such as the adiabatic rapid passage and 180° pulse masers are omitted.

(1) Several masers are already in operation in microwave radiometers. The ability to detect very small temperature changes (on the order of 10^{-2}°K) is one advantage of a radiometer employing a maser preamplifier. Further applications for terrestrial rather than celestial mapping are currently under development.

(2) A secure air to air communication system for use above 15,000 ft. could use the water vapor absorption area near 23 kmc/sec to prevent ground monitoring. Additional advantages accrue from the highly directive antennae available and elimination of muli-path fading.

(3) The same advantages could be applied to a communication system near 60 kmc/sec in the oxygen absorption line. The use of masers would guarantee maximum sensitivity and hence maximum range.

(4) In a tropospheric scatter communication system where the antennae are aimed skyward, a maser could increase the sensitivity of the receiving equipment and thereby reduce the transmitter output power required for an equal reliability factor.

(5) For certain restricted applications a maser could add significantly to the sensitivity of a radar. A reduction of one-fifth in the receiver noise figure (in db) means a theoretical increase in range of 1.5 times the original range [3]

SECTION II

Theory of a Three Level Solid State Maser[1]

A. Introduction

A CW maser utilizes at least three low-lying Zeeman levels of a diamagnetic host crystal containing a fraction of one percent of paramagnetic ions. Arbitrarily numbering the levels 1, 2 and 3 in ascending order, a relatively strong electromagnetic field is applied at the frequency of the 1-3 transition where the energy difference is $E_3 - E_1 = hf_{13}$. See figure II-1(a). This is called the pump frequency. If the original thermal distribution of population of the energy levels is such that after the pump power is turned on, the population of level 3 is greater than level 2, it will be possible to amplify a signal at the frequency of the 3-2 transition. In some cases it may turn out that the population of level 2 is greater than level 1 after pumping. Amplification will then be possible at the frequency of 2-1 transition. When the pump energy is applied continuously, continuous amplification is possible at the frequency of the energy difference between the "inverted" energy levels.

1. [20] & [21] are two very good sources of material on the theory of CW masers. This section relies primarily on the former.

B. Simplified Rate Equation Solutions

The theory contained in this section presupposes a knowledge of electron paramagnetic resonance (EPR). A short explanation of the EPR phenomena may be found in Appendix A.

Assuming the existence of a crystal with three energy levels (Zeeman splitting) as shown in Figure II-1(a), the application of a strong RF field at f_{13} will saturate the 1-3 transition. The energy level populations will readjust to new equilibrium positions with energy levels 1 and 3 having the same number of spins. Depending on the thermal equilibrium population of level 2, a population inversion will occur between levels 3 and 2 or levels 1 and 2 as shown in Figure II-1(c), (d). The saturating energy is called the pump energy and the frequency of the energy difference between the inverted levels is called the signal frequency.

When a weak RF field at the signal frequency is applied to the crystal, more downward transitions than upward transitions will be induced because there are more spins in the upper level. Hence, the spin system may be represented by a negative resistance at the signal frequency since it gives a net amount of energy to the signal.

Using the rate equation approach (as in Appendix A) the pumped equilibrium conditions are described by:

$$\frac{dn_1}{dt} = -\frac{\Delta n_{12} - \Delta N_{12}}{2T_{12}} - \frac{\Delta n_{13} - \Delta N_{13}}{2T_{13}} - W_{13}\,\Delta n_{13}$$

$$\frac{dn_2}{dt} = -\frac{\Delta n_{21} - \Delta N_{21}}{2T_{12}} - \frac{\Delta n_{23} - \Delta N_{23}}{2T_{23}} \qquad (1)$$

$$\frac{dm_3}{dt} = -\frac{\Delta m_{31} - \Delta N_{31}}{2T_{12}} - \frac{\Delta m_{32} - \Delta N_{32}}{2T_{23}} - W_{31}\Delta m_{31}$$

where $\Delta m_{ij} = m_i - m_j$

$\Delta N_{ij} = N_i - N_j$

$W_{ij} = W_{ji}$

T_{ij} = A spin-lattice relaxation time which is a function of levels i and j.

Employing the condition that the population differences must sum to zero (both when pumped and at thermal equilibrium) and also assuming that the 3-2 transition is capable of amplification of a signal f_{32} with transition probability W_{23}, equation (1) may be solved:

$$\Delta m_{32} = \frac{2W_{13}\left(\frac{\Delta N_{12}}{T_{12}} - \frac{\Delta N_{23}}{T_{23}}\right) - \Delta N_{23}\left(\frac{1}{T_{12}T_{23}} + \frac{1}{T_{12}T_{13}} + \frac{1}{T_{13}T_{23}}\right)}{2W_{13}\left(\frac{1}{T_{12}} + \frac{1}{T_{23}} + 2W_{32}\right) + 2W_{32}\left(\frac{1}{T_{12}} + \frac{1}{T_{13}}\right) + \left(\frac{1}{T_{12}T_{23}} + \frac{1}{T_{12}T_{13}} + \frac{1}{T_{13}T_{23}}\right)} \quad (2)$$

If it is now assumed that

$$W_{13} \gg \frac{1}{T_{ij}}$$ (saturated pump transition)

then $$W_{32} \ll \frac{1}{T_{ij}}$$ (unsaturated signal transition)

$$\Delta m_{32} \propto \frac{\frac{\Delta N_{12}}{T_{12}} - \frac{\Delta N_{23}}{T_{23}}}{\frac{1}{T_{12}} + \frac{1}{T_{23}} + 2W_{32}} \quad (3)$$

As long as $W_{32} \ll \left(\frac{1}{T_{12}} + \frac{1}{T_{23}}\right)$ the signal power will have little effect on the population inversion. When W_{32} becomes a significant quantity however, the population difference is reduced, thereby reducing the gain of the maser.

When W_{32} may be neglected, equation (3) can be re-arranged to:

$$\Delta N_{32} = \left[\frac{\frac{T_{23}}{T_{12}} \left(\frac{t_{12}+t_{23}}{t_{23}} \right) - \left(\frac{T_{23}}{T_{12}} + 1 \right)}{\frac{T_{23}}{T_{12}} + 1} \right] \Delta N_{23}$$

The quantity in the square brackets is called the "small signal inversion ratio", R. This factor illustrates two important maser characteristics.

(a) Though the inversion ratio is independent of temperature, ΔN_{23} is inversely proportional to temperature. Therefore, if R is assumed to be a constant, the crystal must be cooled to obtain a very large population difference. Some maser amplifiers have been operated at temperatures higher than liquid helium, but their capabilities are severly limited. [1,2]

(b) Assuming all relaxation times to be equal: $R = \frac{t_{13}}{2t_{23}} - 1$

This equation points out the fact that the pump frequency should be greater than twice the signal frequency for a significant inversion ratio. Again, some recent developments have indicated that this may not be an accurate statement under certain conditions. [3,4,5] In addition, R is further modified by different pumping methods. [6,7]

1. Maiman, T. J. "Proceedings of Quantum Electronics Conference", Bloomingburg, N. Y., Sept. 1959
2. Ditchfield, C., Forrester, P. "Physical Review Letters", 1, 448, 15 Dec 58
3. Bloembergen, Shaperio, Pershen & Artman, "Physical Review", 114, 445, 1959
4. Feher, G., Scovil, H.E.D., "Physical Review", 105, 760, 1957
5. Arams, F., Proc IRE Correspondence 48, 108, 1960
6. Melabs Scientific Report No. 5, 9 October 1959, AFCRC Contract No. AF 19(604)-7071
7. BTL Microwave Solid State Devices, Tenth Interim Report, 15 Aug 59, USADRL, Contract No. DA 36-039sc 73224

C. Magnetic Q Concept of a Cavity Maser

The Q of an arbitrary circuit component is usually defined as the ratio of 2π times the energy stored in the component to the power absorbed by the component per cycle. However, in an amplifier, the power absorbed is a negative quantity. A quantity called the "magnetic Q" of a cavity maser can be defined as:

$$-Q_m = \frac{\omega W \text{ (stored in cavity)}}{-P(\text{absorbed in crystal})} \tag{1}$$

The minus sign is merely a convenience so that Qm is a positive quantity.

The stored energy in any cavity may be written

$$W_{\text{stored}} = \frac{1}{2}\mu_0 \int_V H^2 dV \tag{2}$$

In order to find the power emitted by the crystal (-Pabs), one can start with the differential power:

$$dP = W_{\text{STORED}}\, hf\, \Delta n\, dV \tag{3}$$

Using the induced transition probability from equation (A.5-7) with the maximum value of $g(f) = 2T_2$, equation (3) can be solved.

$$P = \frac{1}{8} hf R \Delta N \langle \omega^2 \rangle \gamma^2 T_2 \int_{\text{crystal vol}} P^2(\psi_1, \psi_2, \psi_3)\, H^2 dV \tag{4}$$

Reciprocal magnetic Q may now be written as

$$\frac{1}{Q_m} = \frac{\hbar}{4\mu_0} R \Delta N \langle \omega^2 \rangle \gamma^2 T_2 \zeta \tag{5}$$

where:

$$\Delta N = \frac{hf}{kT} \frac{N}{(\text{number of levels})}$$

$$T_2 = \sqrt{\frac{1}{3}}\, \frac{1}{\gamma \Delta H}$$

As will be shown later, the maximum voltage gain-fractional band width product ($G^{\frac{1}{2}} \frac{\Delta f}{f}$) is obtained with a maximized reciprocal Qm. Here again, it can be seen that a low temperature is needed for good operation. In addition, the f in the numerator of ΔN indicates better maser performance at higher frequencies, other quantities remaining the same. A crystal with a large dielectric constant would also contribute to a relatively large filling factor. Another interesting point is the fact that Qm is not dependent on the total number of spins, but only on the spin density. There is a limitation, however, on the actual doping percentage due to an unacceptable line broadening and a decrease in T_1. Some recent results have shown that improved maser performance at temperatures above liquid helium may be due to higher paramagnetic ion concentrations (ie $\approx$ 1%) than had been used previously. [1,2]

1. BTL, 9th Interim Report on Microwave Solid State Devices, 15 May 1959, USASRDL, Contract DA 36-039 sc 73224

2. Hoskins, R. H., Ferromagnetic and Paramagnetic Devices Conference, Palo Alto, Calif., 15 Jan 1960

D. A Maser Equivalent Circuit

Since the Q of a cavity near resonance may be described by the $\frac{\omega_c L}{R}$ ratio, a similar ratio may be defined to simplify the previously derived magnetic Q.

$$-Qm = \frac{\omega_0 L}{-R_m} \qquad (1)$$

Again the negative signs are present to indicate net gain of signal energy. Taking into account the various ohmic losses of the cavity and crystal as an R_c, the total negative resistance may be expressed as:

$$-R_m = -R_x + R_c$$

where $-R_x$ describes the negative resistance of the crystal alone. The magnetic Q of the cavity containing the crystal can be written from figures II-2(a) and II-2(b).

$$-\frac{1}{Q_m} = \frac{1}{Q_c} - \frac{1}{Q_x}$$

Normally R_c is extremely small (especially at He temperatures) so that

$$\frac{1}{Q_x} \doteq \frac{1}{Q_m}$$

Some external loading, R_e', must be supplied to cancel the large effective negative resistance of the cavity and prevent oscillations. In the kmc region using waveguide, this can be done through an iris which may be analyzed as an ideal transformer. The turns ratio of the ideal transformer will determine the degree of coupling, so $m^2 R_L = R_L'$ would be the coupled resistance at the cavity or $Q_L = \frac{\omega_c L}{R_L}$

From figure II-3: $\frac{1}{Q_{TOT}} = \frac{1}{Q_L} - \frac{1}{Q_m}$

For stable operating conditions (as an amplifier)

$$Q_m > Q_e \quad \text{or} \quad R_m < R_e$$

Assuming a one port cavity for the signal, the reflected and amplified waves would be identical. The reflection coefficient ρ is defined as $\rho = \frac{-Z_c - Z_L}{Z_c + Z_L}$

$$|\rho| = \frac{R_e + R_m - j(\omega L - \frac{1}{\omega C})}{R_e - R_m + j(\omega L - \frac{1}{\omega C})} = G^{1/2} \tag{2}$$

$\omega L - \frac{1}{\omega C}$ can be approximated by $2\omega_c L \frac{\Delta\omega}{\omega}$ and then the power gain is

$$G = \left| \frac{\frac{1}{Q_e} + \frac{1}{Q_m} - 2j\frac{\Delta\omega}{\omega_c}}{\frac{1}{Q_e} - \frac{1}{Q_m} + 2j\frac{\Delta\omega}{\omega_c}} \right|^2 \tag{3}$$

and at the midband frequency ($\Delta\omega = 0$)

$$G^{1/2} = \left| \frac{\frac{1}{Q_e} + \frac{1}{Q_m}}{\frac{1}{Q_e} - \frac{1}{Q_m}} \right| \tag{4}$$

For high gain the denominator should be very small, but for stable amplification $Q_e < Q_m$. Obviously, Q_e cannot differ from Q_m by a significant amount or the gain will suffer. The technique for obtaining high gain is to reduce the external signal coupling until the system is just stable. Because of this, a cavity maser is very sensitive to changes in the impedance seen by the cavity.

The total Q of the maser may be used to define a bandwidth of the amplifier:

$$\frac{\Delta\omega}{\omega_c}_{3db} = \frac{1}{Q_{TOT}} = \frac{1}{Q_e} - \frac{1}{Q_m} \tag{5}$$

multiplying by equation (4)

$$G^{1/2}\frac{\Delta\omega}{\omega_c} = \frac{1}{Q_e} + \frac{1}{Q_m} \approx \frac{2}{Q_m}$$

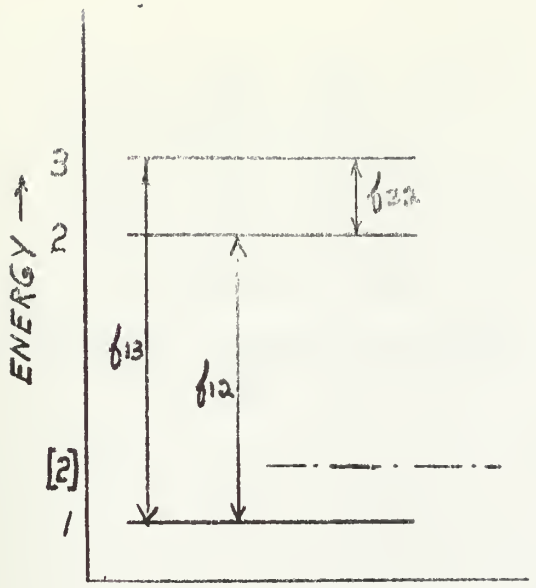

Figure II-1(a)

Separation of energy levels for a constant magnet field

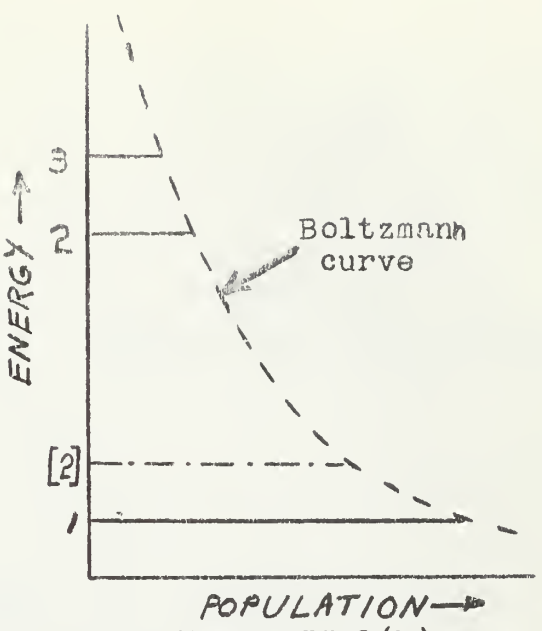

Figure II-1(b)

Thermal equilibrium population distribution

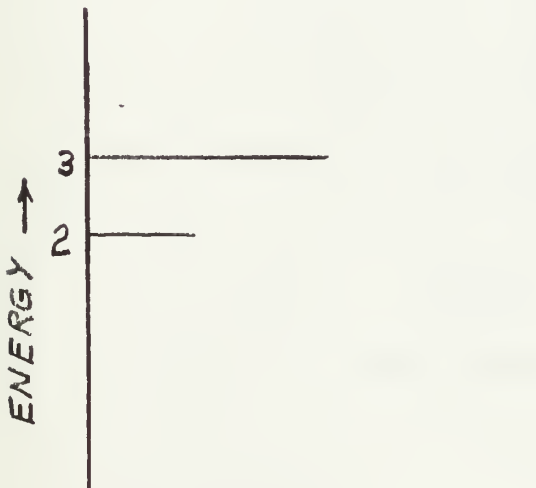

Figure II-1(c)

Inversion of levels 2 and 3

Figure II-1(d)

Inversion of levels 1 and 2

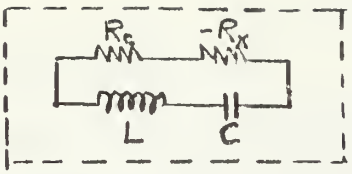

Figure II-2 (a)

Cavity equivalent circuit

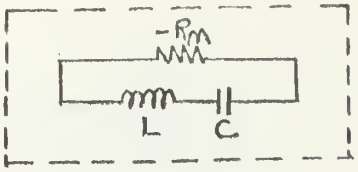

Figure II-2 (b)

Cavity equivalent circuit

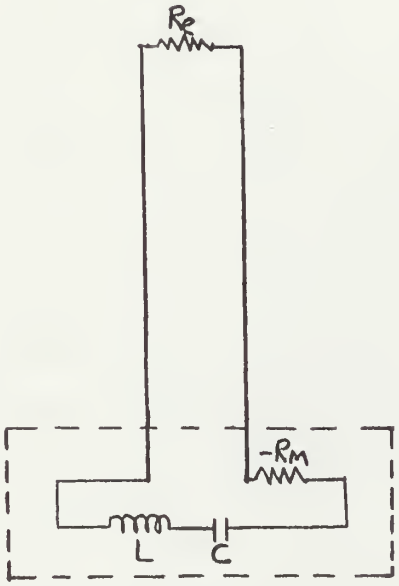

Figure II-2 (c)

Maser equivalent circuit

SECTION III

Description of Equipment

A. The Maser Crystal

In order to utilize paramagnetic resonance [1] in a maser it is necessary for the maser crystal to exhibit a zero field splitting of approximately twice the desired frequency of amplification. This is to obtain a large idler to signal frequency ratio and also from figure III-1 it can be noted that the energy levels are widely separated in the region of $E_{\varphi}/2$. This lends an inherent stability to the device and additionally does not require an excessive magnetic field for comparatively high signal frequencies.

Furthermore, the material chosen must have rugged mechanical characteristics and ability to withstand wide thermal variations. A high dielectric constant is also very helpful in that it provides a longer electrical path within the crystal for maximum interaction of the pump energy with the paramagnetic ions. Long spin-lattice relaxation times are essential to maser operation so that a small average pump power may be used.

Rutile (titanium dioxide), when doped with a paramagnetic ion such as Cr^{+++} or Fe^{+++} in small concentrations, appears to be particularly suitable for high frequency masers. Conveniently, large boules of this material can be grown by the Verneuil flame fusion process and are commercially available[2]. A rutile crystal initially doped with .2% of Fe^{+++} was chosen for this experiment primarily because it was readily available. Unfortunately,

1. See Appendix A
2. Linde Company

there has been no published material on the energy levels in iron doped rutile, although such a project is underway currently at Columbia University.[1] Rutile also has an extremely low loss tangent of approximately .0003 at 24°C which contributes to a high cavity Q.

Some difficulty was anticipated in coupling pump power into a crystal such as rutile with an anisotropic dielectric constant that varies from 173 parallel to the crystaline c axis to 89 along the a axis [13]. To further complicate the problem, the dielectric constant has a negative temperature coefficient of approximately -9×10^{-4}. Therefore, the dielectric constant increases with a decrease in temperature.

B. Thermal Considerations

The thermal conductivity of the wave guide and associated control devices has considerable bearing on the practical design of a maser. A compromise must be made between conservation of helium and an optimum microwave circuit. Furthermore, with the advent of compact and lightweight closed cycle helium cryostats, heat leaks through microwave circuitry will be of paramount concern to the designer.

A calculation of the amount of power (heat) a material will conduct is somewhat complicated by the non-linear characteristic of the thermal conductivity. Stainless steel is a good material for thermal isolation at room temperature and even better at liquid helium temperature, where it has very little thermal conductivity.

1. Private correspondence from Mr. David L. Carter to Mr. Roy W. Roberts of Melabs. See Appendix B

Table I illustrates this [4].

Table I

Temperature (°K)	Thermal Conductivity $\frac{mw}{cm\text{-}°K}$
4°	2.4
40°	47
100°	92
300°	150

However, the electrical conductivity of stainless steel (about one-fiftieth the conductivity of silver) leaves something to be desired. The resulting high losses in stainless steel waveguide may be avoided by silver plating the inside surface of the waveguide to a very small depth (.0005 inches).

The thermal power transmitted by a material is described by the relation

$$P = \sigma A \frac{\Delta T}{\Delta L}$$

Solving this equation when σ is a function of temperature:

$$P = \frac{A}{L}\left[\frac{MT^2}{2} + bT\right]_{T_2}^{T_1}$$

This assumes that σ (t) may be represented by a series of straight lines of the form y = mx + b. It was found that σ (t) could be approximated very closely by only three straight lines:

4° -62°	5/4 T° -2.6
62° -108°	16/31 T° + 40
108° -300°	.3 T° + 62.5

It might be noted that the values of thermal conductivity used in these calculations is for type 347 stainless, which is chemically very similar to the type 304 stainless used in constructing the maser to be described.

By assuming that the nitrogen jacket cools the maser assembly to about 108°K at a point one-half way down the inner dewar to the helium level, (after one-half of the helium has boiled away) one can predict that it will take about 3 hours and 25 minutes for the helium to completely boil away. This also assumes that the average boil-off rate is at the point where the helium is one-half evaporated. In practice the helium was found to last for over five hours. Some of the liquid remaining in the inner dewar was liquid oxygen, but it is impossible to say just how much. The helium loss is much less than calculated, even though only an order of magnitude calculation was intended.

C. Microwave Circuitry

The entire microwave assembly was enclosed in a glass dewar of 1.75" ID. This inner dewar was then inserted inside another dewar of about 2.5" ID. Liquid nitrogen (77°K) filled the space between the inner and outer dewar and liquid helium (4°K) was forced into the inner dewar. See figures III-2 through III-5.

The larger signal waveguide (RG-96/U) has inside dimensions of .140" X .280" while the pump waveguide (RG-98/U) is almost exactly one-half this size. Both types are made of coin silver with .040" wall thickness.

Initially, the circuitry of this maser was unique due to one innovation. It was a cavity maser without a physical cavity. Instead, the signal waveguide was merely terminated in the rutile

crystal which completely filled the end of the pump waveguide and an E-H tuner was used to provide the variation in coupling required at the signal frequency. This circuit worked very well for the resonance observations required to make the iso-frequency plots, but the E-H tuner did not produce the desired decoupling effects during the first masering attempts.

The tuning plungers of the E-H tuner were of the fairly common dumbell type. They were fabricated from brass which was subsequently silver coated. Calculations indicate that the short lengths of RG-96/U were terminated in less than one-tenth their characteristic impedance by the plungers. The plungers were soldered directly to long stainless steel rods which were threaded through the 1/4" brass top plate. Three quarters of an inch of thread on the rods allowed ample tuning over about two wave lengths at the signal frequency. Commercially available cast bends[1] were used to get the E-H tuner into the longitudinal axis so the vertical stainless steel control rods could be employed. In the signal circuit, thermal isolation was obtained with a 22" piece of stainless steel waveguide with .010" walls.

The RG-96/U waveguide was terminated 1.5" below the E-H tuner by butting it against a hooked section of RG-98/U. The rutile crystal (.148" X .074" X .400") was inserted directly into the end of the RG-98/U and projected up into the RG-96/U. The pump energy was passed through a section of stainless steel tubing (.120" ID X .200 OD) six inches long. This was used because no

1. Microwave Development Laboratories

rectangular stainless guide similar to RG-98/U was available. Transitions to the circular modes were made by tapering the rectangular RG-98/U waveguide to a circular cross-section of about .160" diameter. The stainless tube was also bored out to equal this diameter. These transitions were each about 3/4" long.

Calculations were made to see if it would be advisable to silver plate the interior of the sections of stainless waveguide. For a 24" section of stainless RG-96/U, a 2 db improvement could be realized by silver plating. Since signal power was not a problem, the improvement did not warrant the additional cost and the RG-96/U was left un-plated. However, due to the 6.5 db insertion loss of the pump transmission line, it was decided to attempt to silver plate the six inch stainless tube. This was at least partially successful since the insertion loss was reduced to 4.5 db. Unfortunately, the insertion loss of the stainless section was a function of the angle at which the wave was launched into the circular mode. The two sections of RG-98/U at each end of the stainless tube had to be offset by about 20° to obtain maximum power transfer. This offset angle indicated that some type of frequency sensitive mode rotation was occuring in the transitions and hence modes other than the desired TE_{11} were being propogated. Therefore, maximum power transfer could take place at only one frequency and pump tuning would be very difficult.

To overcome these disadvantages a three inch section of stainless steel RG-96/U terminated at each end with one inch tapered transitions from RG-98/U was used instead of the stainless tube. Even though it increased the chances of generating higher order modes, this configuration reduced the pump waveguide insertion loss to 2.7 db.

Some further modifications to the microwave structure were made in the later phases of the experiment and they will be described in another section.

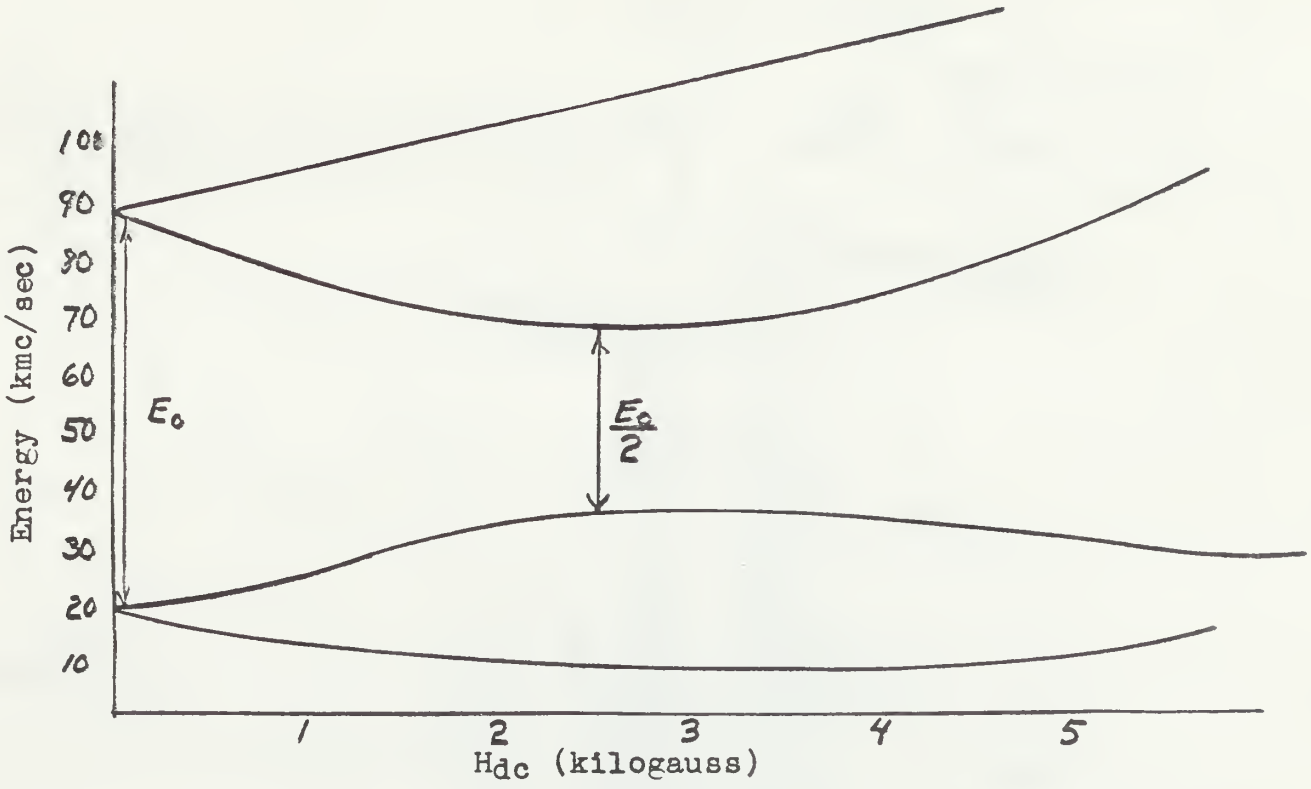

Figure III-1

Energy levels in an arbitrary crystal

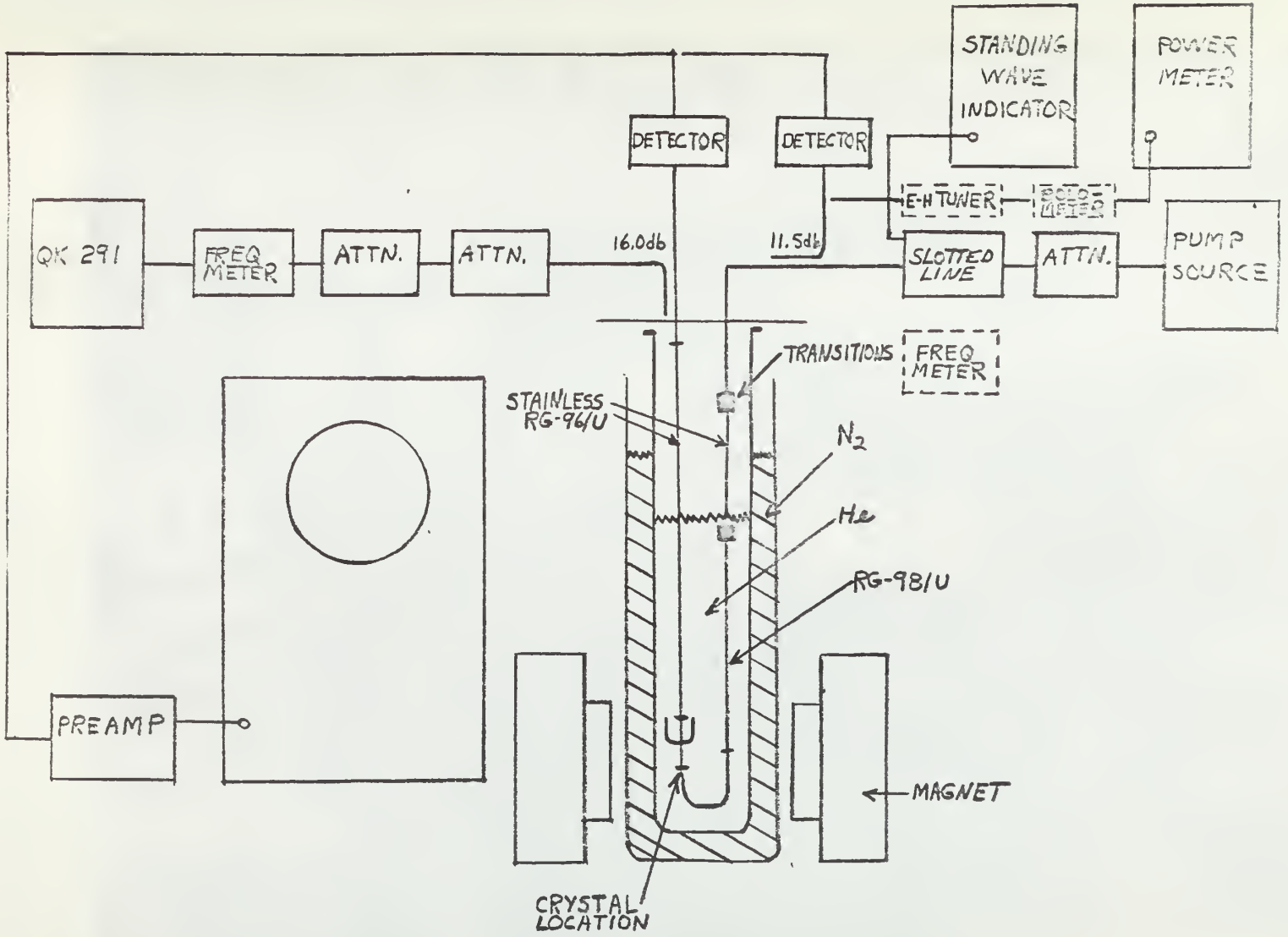
STANDING WAVE INDICATOR
POWER METER
DETECTOR
DETECTOR
E-H TUNER
QK 291
FREQ METER
ATTN.
ATTN.
16.0db
11.5db
SLOTTED LINE
ATTN.
PUMP SOURCE
TRANSITIONS
FREQ METER
STAINLESS RG-96/U
N_2
He
RG-98/U
PREAMP
MAGNET
CRYSTAL LOCATION

FIGURE III-2

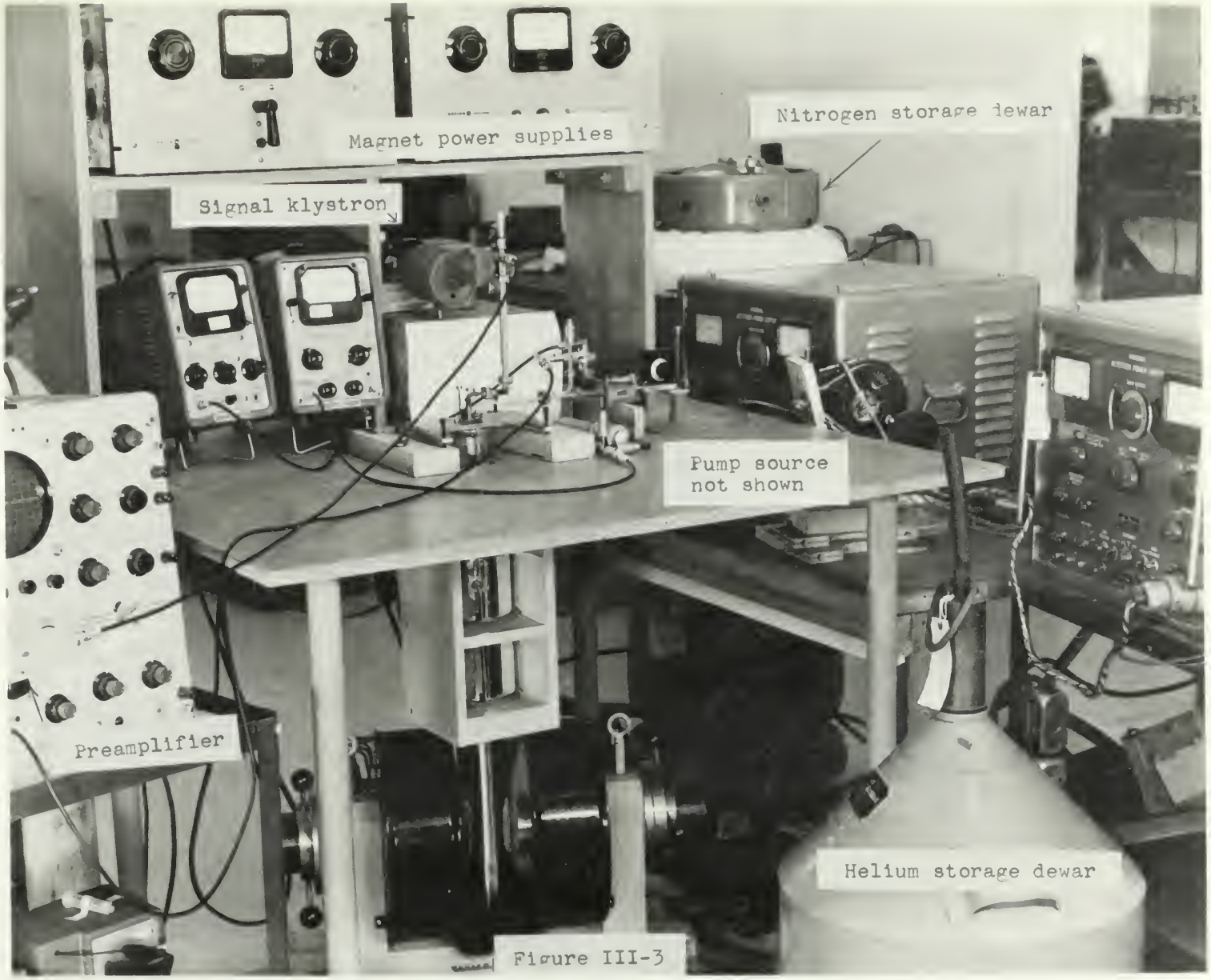
Magnet power supplies
Nitrogen storage dewar
Signal klystron
Pump source
not shown
Preamplifier
Helium storage dewar

Figure III-3

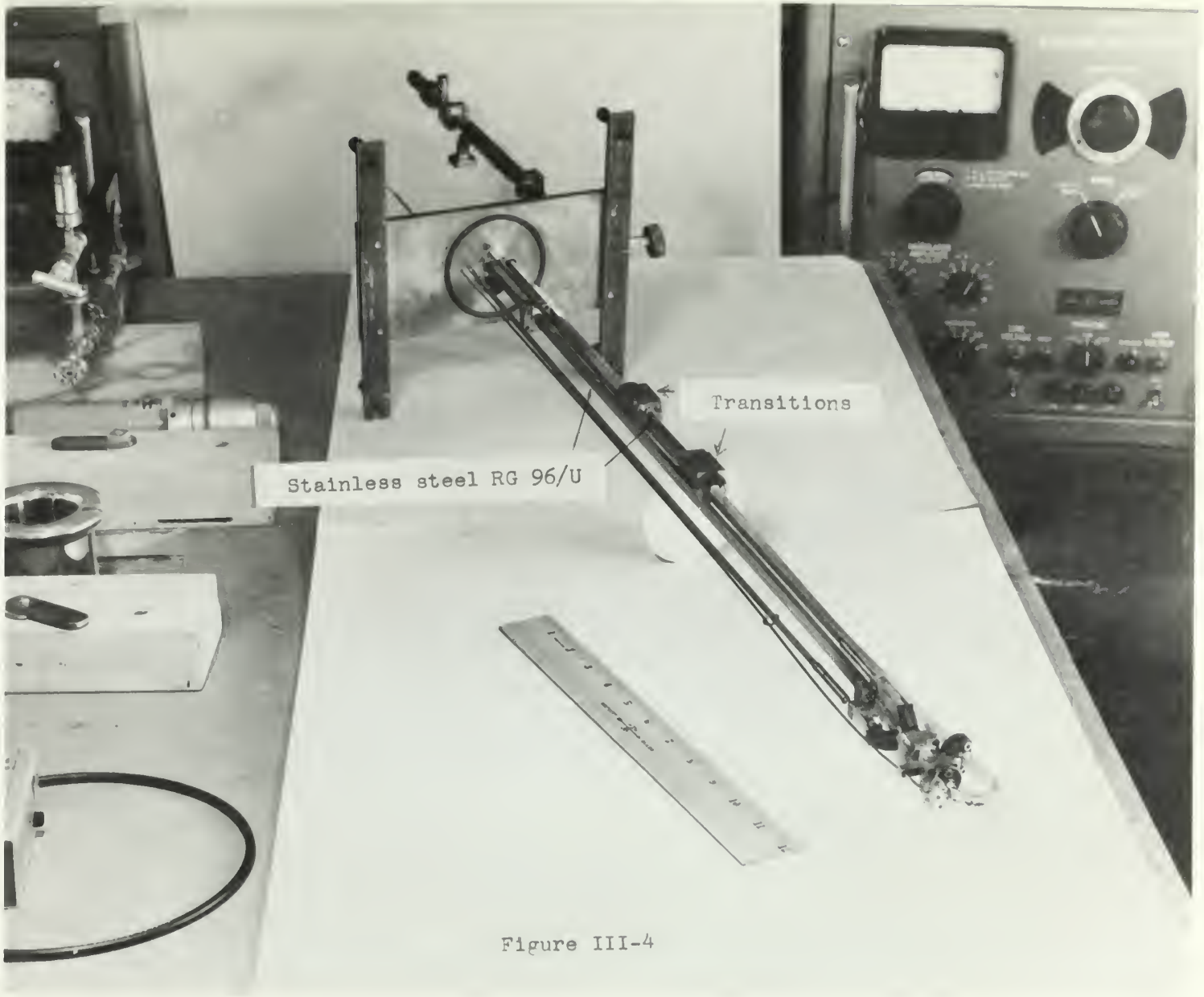

Figure III-4

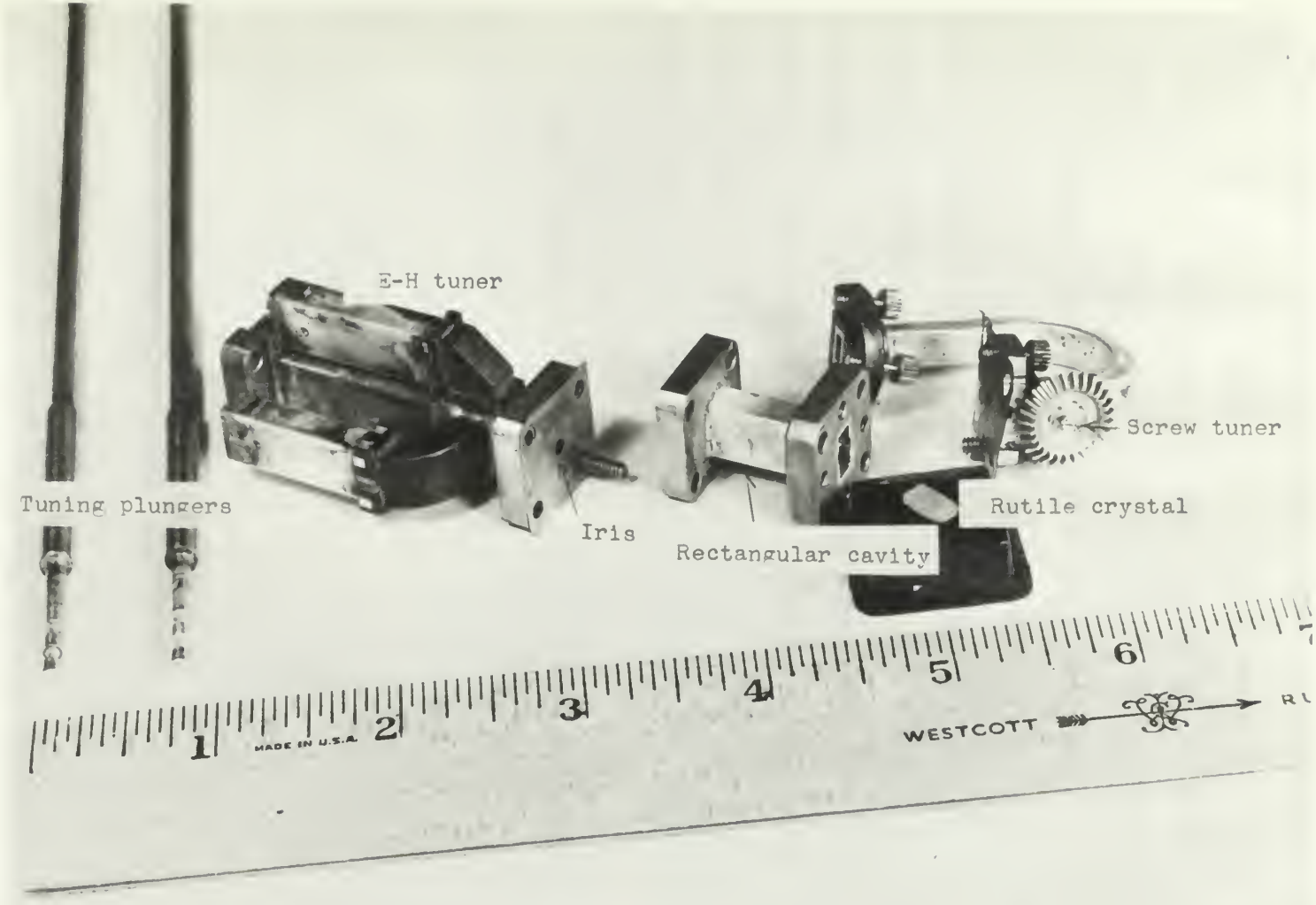
E-H tuner
Tuning plungers
Iris
Rectangular cavity
Rutile crystal
Screw tuner
MADE IN U.S.A.
WESTCOTT

Figure III-5

SECTION IV

Experimental Results

Maser design using rutile is complicated considerably by the absence of energy level diagrams. There are design procedures that bypass this difficulty, but they are time-consuming and suffer from an inherent degree of randomness. The method chosen in this experiment was to construct iso-frequency plots. An iso-frequency plot is a graph of paramagnetic resonances at a constant signal frequency plotted vs. applied magnetic field at various angles. The crystalline c axis is used as the reference line in determining the orientation of the magnetic field. The intersection of a pump resonance line with a signal resonance line indicates a possible masering point. However, maser action is not possible if the pump transition does not include the signal transition. See figure IV-1.

Iso-frequency plots were made at the following frequencies with essentially the same set-up as shown in figure III-1.

Frequency	Temperature
26.90 kmc/sec	77 °K
28.03 "	77 "
29.90 "	77 "
30.00 "*	4 "
35.00 "*	77 "
42.62 "	4 "
67.45 "*	4 "
69.35 "*	77 "
75.00 "	4 "

Plots marked with an asterisk are included as figures IV-2 and IV-3. The lines connecting the resonance points are merely the

author's conjecture of a possible energy level distribution and may not be an accurate portrayal of the actual distribution. A photograph of an oscilloscope display of paramagnetic resonance at pump and signal frequencies is shown in figure IV-4(a), (b).

With the information available from the iso-frequency plots and from [22], several unsuccessful attempts were made to obtain maser action in the vicinity of 0° and 3000 gauss. As a result of these attempts, some changes were made in the microwave circuitry.

There appeared to be two plausible reasons why the system was not operating properly;

(a) the crystal was not being saturated due to improper coupling or insufficient pump power.

(b) the E-H tuner was not creating a cavity in the section of RG-96/U of sufficiently high Q to neglect the R_c losses and allow the effective negative resistance of the crystal to cause amplification.

Considerable pump power was being reradiated by the crystal into the signal waveguide. Ample evidence of this is shown in figure IV-4(b) where the reflected signal power roughly appromimates the transmitted pump power. In order to improve the interaction of the pump power with the spin system, the crystal was silver coated with the exception of about 1/8" at the junction of the RG-98/U and RG-96/U wave guides where there would be strong signal magnetic fields. Resonances were very difficult to observe at both pump and signal frequencies with the silver coating as described. The original

coating of silver was removed with nitric acid and another applied allowing about 1/4" for signal coupling to the crystal. Again, it was practically impossible to note signal resonance effects. This coating was removed with the exception of the top surface of the crystal which, it was hoped, would reflect some of the pump power back through the crystal. In addition, the end of the crystal that fitted into the pump waveguide was ground down to a taper about .080" long. During this process the crystal chipped, resulting in a new overall length of .320". The smaller volume of the crystal was actually an advantage since it reduced the amount of saturating power required.

Using the tapered crystal as a matching device was unsatisfactory, so a tuning screw was put into the pump waveguide as close to the crystal as possible. Room temperature experiments indicated that the VSWR in the pump waveguide could be kept below 1.5 for a constant screw position over a band width of about 500 mc/sec. Encouraged by these results, it was planned to leave the pump at a fixed frequency with the screw tuned for minimum VSWR (maximum power transfer) at room temperature and use the signal frequency and magnetic field as the variables to find a double resonance. Signal and pump interactions were noted, but again no gain could be observed.

Two runs were made to see if the crystal was actually being saturated by the pump. These were accomplished by observing the

reflected pump power from the crystal and screw. As the pump power was reduced by small increments, a change in the slope of the reflected power curve would indicate a change in the power absorption or susceptance characteristics of the crystal such as one finds near the saturation level. This data was inconclusive since the rapid change in slope occurred before .5 db of attenuation was placed in the pump waveguide and might have been due to pulling effects on the pump klystron.

A tuning control for the screw tuner was devised so that it could be operated from the top of the apparatus. Another run was made and as before, interaction of pump and signal was evident in several places, but no gain was observed.

By this time it was apparent that the E-H tuner was not providing the isolation and decoupling required. Therefore, it was decided to create a physical cavity and hence increase the effective Q. The signal waveguide was cut and flanged just below the E-H tuner. Shim copper irises were made to be inserted at the top and bottom of the small (.8") section of RG-96/U containing the crystal to provide signal and pump coupling respectively into the rectangular cavity. See figure III-5.

At this point it was also decided to change the orientation of the crystal c axis with respect to the pump magnetic field. Heretofore, the two were perpendicular because the crystal c axis was perpendicular to the wide side of the crystal. Two

grooves were filed into the sides of the rectangular cavity of RG-96/U to accomodate the crystal in its new position.

Room temperature experiments were made to find an optimum size for the irises. Diameters of .100" and .075" were chosen for the signal and pump respectively. With this arrangement, the E-H tuner had a pronounced effect, and some gain was observed as shown in figure IV-4(c). However, in this case, the signal klystron was pulse modulated in an attempt to reduce average signal power. Further experiments were made with irises of .063" for signal and .060" for pump. Cavity resonances at signal frequencies were much harder to observe than in the prior attempt and the E-H tuner did not decouple the signal properly.

In the final experiment the pump iris was removed and the pump waveguide rotated 90° so that the pump and signal waves in the cavity were orthogonal. The signal iris was also increased slightly to .075" diameter. Here again positive interaction was obtained as shown in figure IV-4(d).

Some explanation should be made of the value of magnetic field taken as causing resonance. Resonance was marked by the appearance of a cavity and crystal absorption dip on the 60 mc/sec frequency modulated klystron mode. As the magnetic field was increased slightly, the absorption dip or dips would travel across the mode in the direction of increasing frequency and reappear at about their original position when the field had traversed the resonance

line. The magnetic field at the midpoint of the traverse of the absorption dip was taken as the resonant field. Line widths seemed to vary considerably with an average being in the neighborhood of 40 gauss.

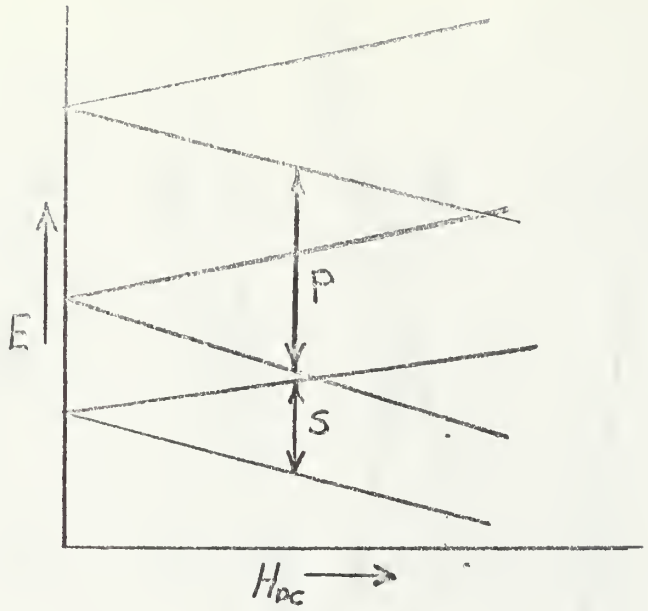

No maser action possible

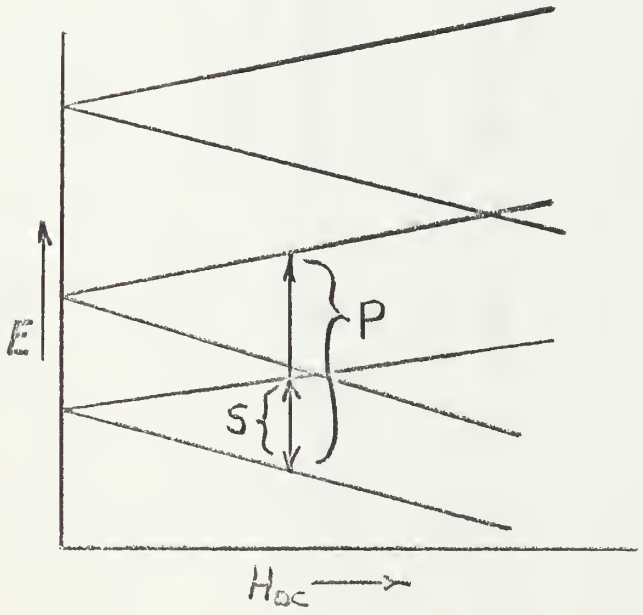

Maser action possible

Figure IV-1 Possible crystal resonances derived from an iso-frequency plot

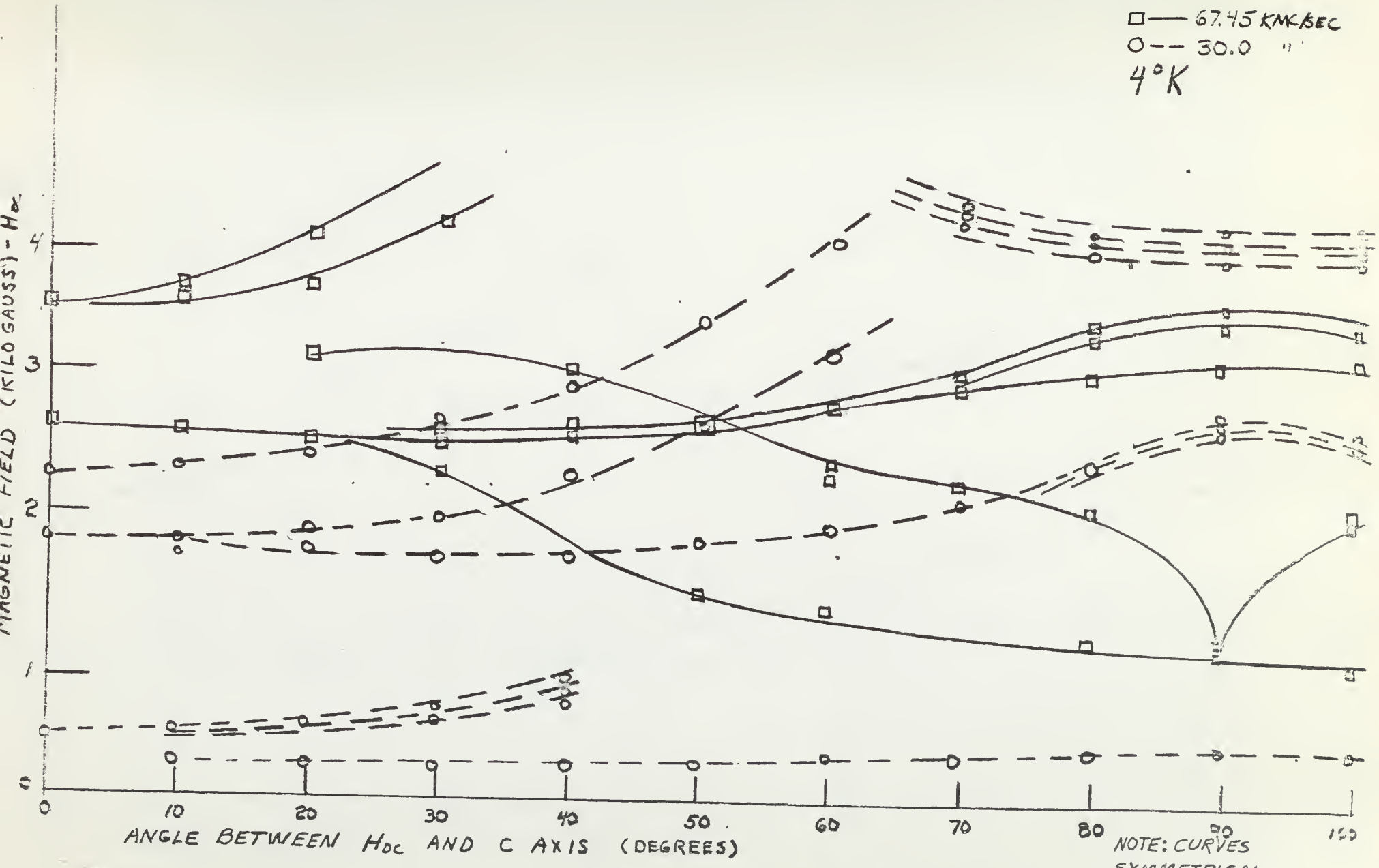
□— 67.45 KMC/SEC
O-- 30.0 "
4°K
MAGNETIC FIELD (KILO GAUSS) - H_{dc}
4
3
2
1
0
0
10
20
30
40
50
60
70
80
90
100
ANGLE BETWEEN H_{DC} AND C AXIS (DEGREES)
NOTE: CURVES SYMMETRICAL ABOUT 90°

FIGURE IV-2

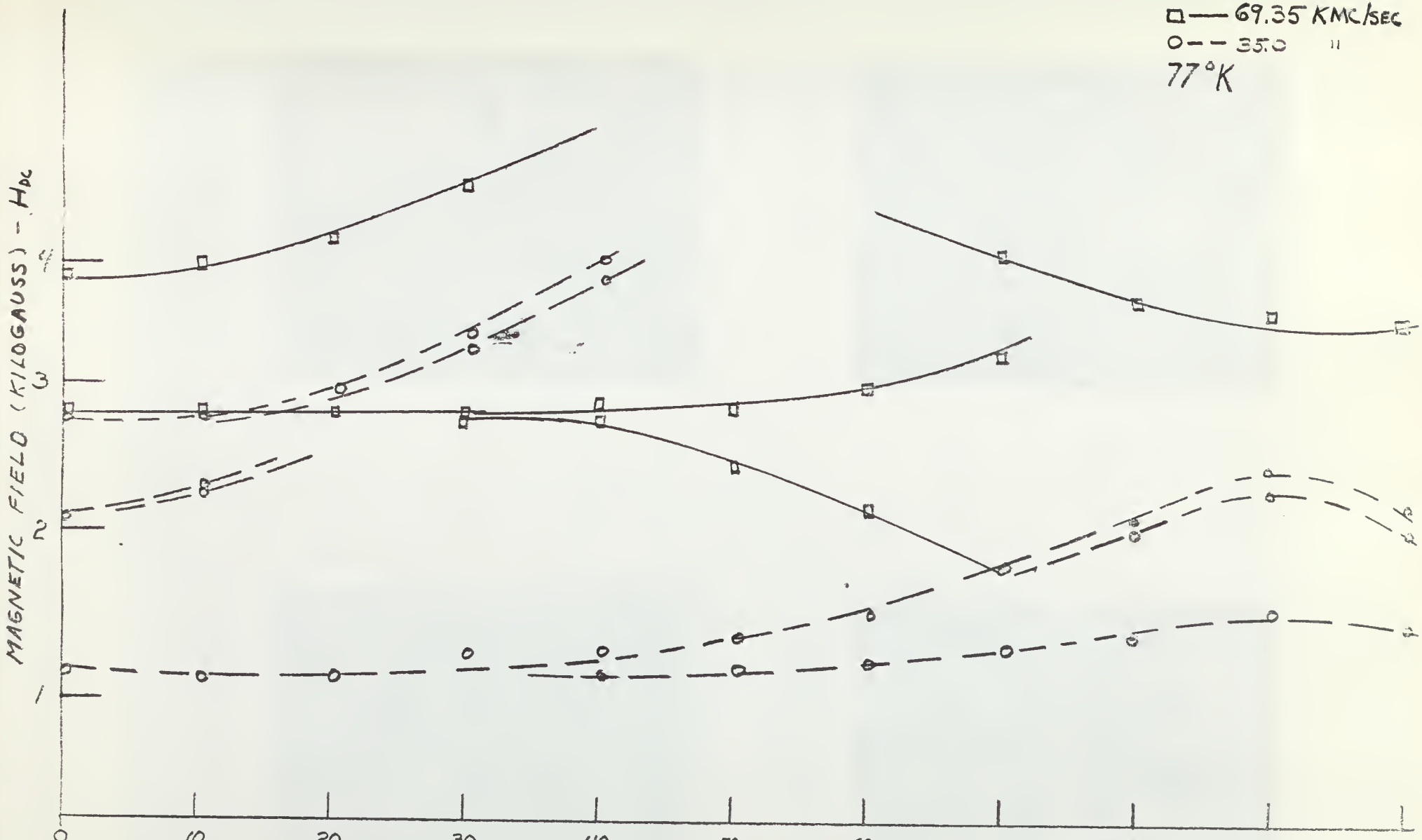
□ — 69.35 KMC/SEC
○ - - 35.0 "
77°K
MAGNETIC FIELD (KILOGAUSS) - H_{dc}
3
2
1
0
10
20
30
40
50
60
70
80
90
100
ANGLE BETWEEN H_{dc} AND C AXIS (DEGREES)
NOTE: CURVES SYMMETRICAL ABOUT 90°

FIGURE III-3

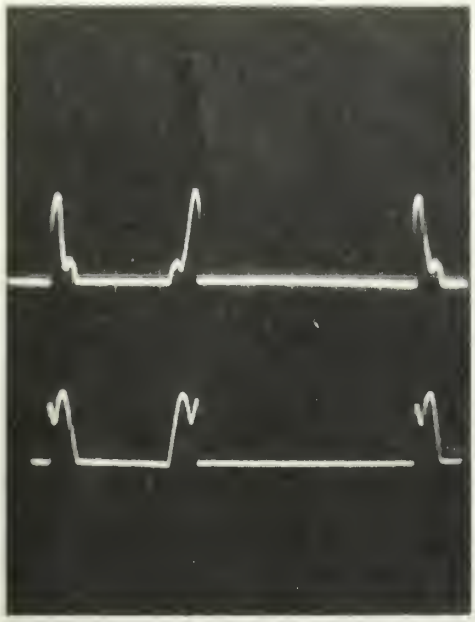

Magnetic field off

Magnetic field on

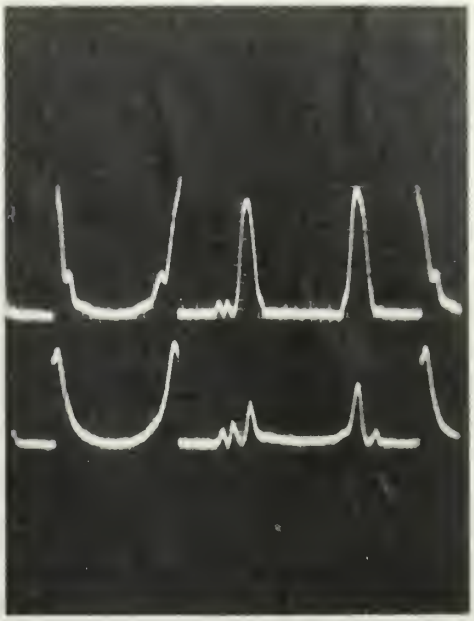

(a) Resonance at 36.2 kmc/sec, 0°, 3.4 kilogauss

(b) Simultaneous resonance at 36 kmc/sec and 70.1 kmc/sec, 0°, 3.2 kilogauss

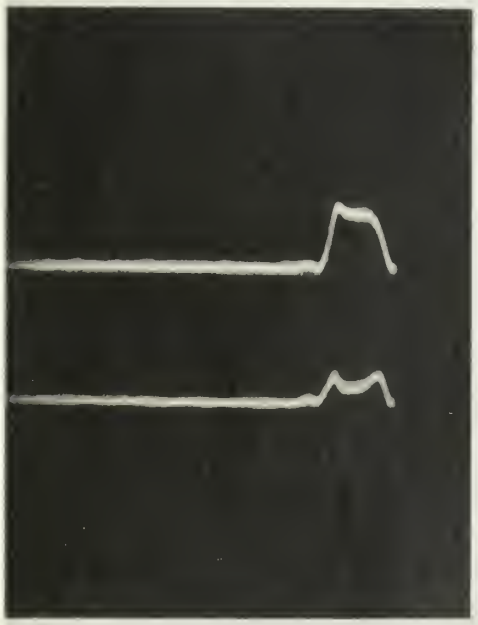

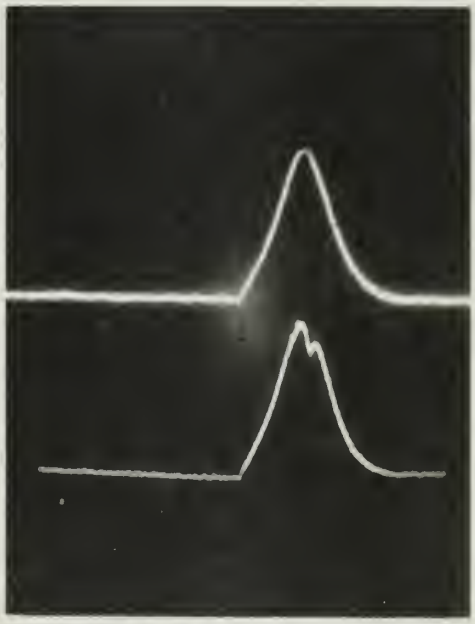

(c) amplification of pulsed signal at 36 kmc/sec. Top line pump on; bottom line pump off.

(d) Pump and signal interaction. Top line pump off; bottom line pump on.

Figure IV-4

SECTION V

Conclusions

A. General

From the data gathered, it appears that little additional effort is required to produce a fully operable cavity maser in this region. Pump power is a problem, but not as serious as it once seemed since other investigators have observed saturation effects with 2-10 mw incident on a more sophisticated cavity [22]. As soon as energy level diagrams become available, design problems will be simplified and the desired operating orientations can be forecast accurately.

B. System Considerations

The one great advantage of a maser preamplifier in the microwave region is, of course, the extremely small amount of noise that is generated within the amplifier. In fact, it is very difficult to design (or redesign) a microwave system that will utilize a reasonable portion of the potential increase in system sensitivity due to a maser. As noted in Appendix C, the noise temperature of the first device in a cascaded series contributes a significant portion of the overall noise temperature of the system. An antenna pointing at the "coolest" part of the sky and in the most favorable frequency range (2-10 kmc/sec) has a noise temperature greater than that of the maser. If we assume, optimistically, a receiver with a noise temperature of about 2000 °K connected to this antenna,

the addition of the maser increases the system coherent signal sensitivity by over 20 db. However, when the antenna is looking at the earth, a 290°K source, the addition of the maser contributes only about 8 db additional sensitivity to the system. In some applications the additional 8 db might be worth the disadvantages attendent upon installing a maser.

Undoubtedly the most serious of these disadvantages is the present requirement for liquid helium. Liquid nitrogen or air is also used in most installations for precooling to conserve helium. Due to the interest shown in maser development, a closed cycle liquid helium system is currently in the final stages of development and should be available soon. This will remove one large roadblock in the path of maser system applications.

Laboratory installations use a large external electromagnet in experimental set-ups, but a small permanent or super-conducting electromagnet can be substituted in specific applications. In addition, a stainless steel dewar flask can be used instead of the more fragile pyrex glass dewar usually found in the laboratory.

Some difficulty has been encountered in attempting to install a maser preamplifier in pulsed radar systems. The large amount of output power creates a requirement for an extremely effective isolating device to prevent the maser from being saturated by leak-through power.

One other drawback to the use of a maser is the requirement for a pumping energy source (faintly analogous to the power supply of a conventional amplifier) of a higher frequency than the signal to be

amplified. However, recent advances in the art have shown that this restriction is not necessarily true for certain configurations of the crystal and equipment.

As with most amplifiers in the microwave region, bandwidth times voltage gain is a constant in a maser. A cavity maser at X-band might have a gain of 15 db over a 15 mc bandwidth. A traveling wave maser usually has a broader bandwidth with the additional advantage that the gain is directly proportional to the length of the slow wave structure.

BIBLIOGRAPHY

1. N. Bloembergen, "Physical Review" 104, 324 1956

2. Harold I. Ewen, "the microwave journal" 2, 41 1959

3. J. R. Singer, "Masers" Wiley & Sons 1959

4. Russell B. Scott, "Cryogenic Engineering" Van Nostrand 1959

5. Gordon Troup, "Masers" Methuen & Co. London 1959

6. William From, "the microwave journal" 1 18 1958

7. Theodore Moreno, "Microwave Transmission Design Data" Dover 1948

8. S. Ramo and J. Whinnery, "Fields and Waves in Modern Radio" Wiley 1953

9. Procedings of the Symposium on Solid State Masers, 12-13 June 1958, Fort Monmouth, N. J. U. S. Army Signal Research and Development Laboratory

10. Gerritsen, Harrison, Lewis, Wittke, "Fine Structure, Hyperfine Structure, and Relaxation Times of Cr^{+++} in TiO_2 (Rutile)" Phys. Rev. Ltrs 2, 153 15 Feb 59

11. DeGrasse, Schulz-DuBois, Scovil, "The Three Level Solid State Traveling Wave Maser" B S T J XXXVIII 305 1959

12. Schulze-DuBois, Scovil, DeGrasse, "Use of Active Material in Three Level Solid State Masers" B S T J XXXVIII 335 1959

13. F. A. Grant, "Properties of Rutile" Rev. Mod. Phy. 31 647 1959

14. D. C. Hogg and W. W. Mumford, "The Effective Noise Temperature of the Sky", the microwave journal, 3 80 1960

15. P. N. Butcher, "Theory of CW Solid State Masers" Stanford Electronics Laboratories, Technical Report No. 155-1. 16 Dec 57

16. W. S. C. Chang, J. Cromack, and A. E. Siegman, "Cavity and Traveling Wave Masers using Ruby at S-Band", Proc. PGAP and PGMTT 1959 IRE WESCON

17. H. D. Tenney, R. W. Roberts, and P. H. Vartanain, "An S-Band Traveling Wave Maser", Proc. PGAP and PGMTT 1959 WESCON

18. Westinghouse Research Laboratories, "Maser Studies" Quarterly Technical Reports 1 through 10, AF, WADC contract # AF33(616) 5258

19. Melabs Inc., "Research and Development of a Solid State Paramagnetic Maser", Quarterly Progress Reports 1, 2, 3, 5, AFCRC contract AF 19(604)-4071

20. A. E. Siegman, "Solid State Masers" To be published by McGraw-Hill

21. J. O. Artman, Cruft Laboratory Technical Report 264, Navy Contract Nonr-1866(28) Nr-372-012

22. S. Foner & L. R. Momo, MIT Lincoln Laboratory Report, M82-16, "A CW Millimeter Wave Maser", 16 December 1959

Appendix A

Paramagnetic Resonance[1]

1. Introduction

It might be well to begin this section with some basic definitions:

(a) Paramagnetism is ascribed to the tendency of certain atoms to exhibit a magnetic moment in the direction of an applied field.

(b) Diamagnetism results from a minor modification of the quantum states producing a very slight magnetic moment in a direction opposed to an applied field.

(c) Ferromagnetism is a phenomena resulting from an alignment of electron spins in separate atoms under special conditions.

Transition group elements are the only common materials that exhibit paramagnetic susceptibility. However, due to the close proximity of atoms in a crystal ($\approx$ 10 Angstroms), paramagnetic ions are constantly acted upon by the randomly fluctuating fields of their neighbors. These fields are on the order of 100 gauss. In order to reduce this inter-ion coupling, paramagnetic salts used in masers are usually diluted. This is accomplished by

1. This section generally follows a similar but more detailed treatment in some course notes of Professor A. E. Siegman of Stanford University. With additions, and under the title, Solid State Masers, these notes are to be published by McGraw-Hill.

inserting a small percentage of the paramagnetic ions in a non-magnetic host crystal. Naturally, this is possible only when the magnetic and nonmagnetic substances have the same ionic value and approximately the same size so that either ion can interchangeably occupy a particular site in the crystal structure. Such a process is called "doping" a crystal.

An ion in a crystal acts as if all of its magnetism is the result of its spin angular momentum. None appears to be produced from the orbital angular momentum. This may be attributed to the strong crystalline electric fields and the resulting Stark splitting of the ionic energy levels. Contrary to the $2J + 1$ magnetic levels one finds in a free ion, a common result is that $2S + 1$ levels separated by $\Delta E = gBH$ where $g = 2$, the spin-only value, instead of $g = g_j$, the Lande factor. The S referred to above is "effective spin" and is in many cases equal to the free ion spin.

Consider an isolated paramagnetic ion which has an $S = 1/2$. There are only two energy states possible, $+1/2$ and $-1/2$. These levels will vary with the applied magnetic field as shown in figure A-1. The numbers of spins (or ions) in each state will be distributed according to a Boltzmann distribution. See figure A-2.

Now, if the crystal is exposed to an RF field of the correct frequency, the electrons will be stimulated to jump back and forth between the energy levels. This frequency is defined by

$$\omega_{12} = \left(\frac{gB\mu_0}{\hbar}\right) H_0 \qquad (1)$$

When a quantity γ is set equal to the quantity in the parenthesis of equation (1)

$$f_{12} = \frac{\gamma}{2\pi} H_o$$

For an electron, with $g = 2$

$$\frac{\gamma}{2\pi} = 2.8 \text{ mc/gauss}$$

Therefore, one can see that for a magnetic field, H_o, on the order of several thousand gauss, transition frequencies in the kilomegacycle/sec region may be expected.

2. Rate Equations

Probably the simplest way to construct a model of paramagnetic resonance is to utilize the rate equation approach. These equations describe a spin system by defining the number of spins in each energy level. With the rate equations one can show how the average values of energy level populations vary with time. The time variations may be due to an internal relaxation process or to energy absorbed from an external signal.

Consider a lightly doped crystal where the paramagnetic ions may be assumed to be nearly independent and, as in the previous section, $S = \frac{1}{2}$. At thermal equilibrium the Boltzmann distribution of the populations of the energy levels is

$$\frac{n_2}{n_1} = \frac{N_2}{N_1} = e^{-(E_2 - E_1)/kT} \tag{1}$$

when $\Delta E = E_2 - E_1 = h f_{12}$, equation (1) may be rewritten

$$\frac{N_2}{N_1} = e^{-hf_{12}/kT} \approx 1 - \frac{h f_{12}}{kT} \tag{2}$$

The implicit assumption is that $hf_{12}/kT \ll 1$. At frequencies below about 10 kmc/sec this is completely valid, but above this frequency the second order effects may be appreciable. To keep this approach simple, assume the former case exists. Another condition that must exist is:

$$n_1 + n_2 = N_1 + N_2 = N \tag{3}$$

Taking into account the small population difference one can write

$$N_1 \approx \frac{N}{2}\left[1 + \frac{h f_{12}}{2kT}\right]$$

$$N_2 \approx \frac{N}{2}\left[1 - \frac{h f_{12}}{2kT}\right] \tag{4}$$

and

$$N_1 - N_2 = \Delta N = \frac{h f_{12}}{kT}\frac{N}{2}$$

Since the spin system is in contact with the crystal lattice there will be occassional transitions caused by thermal fluctuations of the crystal. To describe this action

$$\frac{dn_1}{dt} = -w_{12} n_1 + w_{21} n_2 \tag{5}$$

$$\frac{dn_2}{dt} = w_{12} n_1 - w_{21} n_2 \tag{6}$$

where $\frac{dn_1}{dt}$ = change in population of level 1 with time

and at thermal equilibrium

$$\frac{dN_1}{dt} = -w_{12} N_1 + w_{21} N_2 = 0 \tag{7}$$

$w_{21} > w_{12}$ since $N_1 > N_2$ due to the Boltzmann distribution. The transition probabilities are usually written as shown below with T_1 being a quantity with time dimensions:

$$w_{12} = \frac{1}{2T_1} e^{-\frac{hf_{12}}{2kT}} \approx \frac{1}{2T_1}\left[1 - \frac{hf_{12}}{2kT}\right]$$

$$w_{21} = \frac{1}{2T_1} e^{+\frac{hf_{12}}{2kT}} \approx \frac{1}{2T_1}\left[1 + \frac{hf_{12}}{2kT}\right] \tag{8}$$

If one can imagine that the populations are in some way redistributed from thermal equilibrium

$$\frac{d(\Delta n)}{dt} = \frac{d(n_1 - n_2)}{dt} = 2(w_{21} n_2 - w_{12} n_1)$$

Using equations (4) and (8)

$$\frac{d(\Delta n)}{dt} = -\frac{\Delta n - \Delta N}{T_1} \tag{9}$$

or

$$\Delta n = \Delta N + \left[\Delta n_{t=0} - \Delta N\right] e^{-\frac{t}{T_1}} \tag{10}$$

Equation (10) shows that the populations will return to thermal equilibrium with an exponential time constant T_1. T_1 is commonly called the spin-lattice relaxation time. This time is

a very strong inverse function of temperature. It is also somewhat dependent upon the energy difference between the ground state and the first excited state with a longer relaxation time occurring the larger the energy difference. T_1 may be anywhere from one to several hundred milliseconds at liquid helium temperature for a maser material.

3. Stimulated transitions

Let W_{12} be the induced probability of a transition caused by an applied RF field. Now equations (5) and (6) of the previous section can be modified to:

$$\frac{dn_1}{dt} = -w_{12} n_1 + w_{21} n_2 + W_{12}(n_2 - n_1)$$

$$\frac{dn_2}{dt} = w_{12} n_1 - w_{21} n_2 + W_{12}(n_1 - n_2) \qquad (1)$$

W_{12} is proportional to the square of the RF magnetic field and it is also the same in either direction ($W_{12} = W_{21}$). As you would expect, W_{12} is maximum when the frequency of the applied RF field is equal to f_{12}. For the $S = 1/2$ transition with the RF and DC magnetic fields magnetic fields mutually perpendicular:

$$W_{12} = \left(\frac{\pi g B \mu_0}{2h}\right)^2 H_{12}^2 g(f) = \frac{1}{16}(\gamma H_{12})^2 g(f) \qquad (2)$$

where

$$g(f) = \frac{2T_2}{1 + T_2^2(\omega - \omega_{12})^2} \qquad (3)$$

and T_2 = spin-spin relaxation time, ie: the time required for energy put into one portion of the resonance line to spread throughout the line.

When $g(f)$ is maximum ($\omega = \omega_{12}$):

$$W_{12} = \frac{1}{8}(\gamma H_{12})^2 T_2 \qquad (4)$$

This value for W_{12} is correct only if the RF and DC fields are perpendicular. There is actually a $\sin^2\Theta$ response involved where Θ is the angle between the fields. Naturally, the problem is more complicated when several energy levels are involved.

4. Line Width

Line width is usually expressed in gauss or megacycles. In a simple experiment it can be measured by looking at the reflected power from a cavity containing the paramagnetic specimen. Referring to figure A-3, the points where the reflected power is one-half of its minimum value can be used to measure line widths.

From equation (A. 3-3)

$$g(f) \sim \frac{1}{1+T_2^2 \Delta\omega^2} \qquad \text{where } \Delta\omega = \omega_1 - \omega_2$$

The power response of a tuned circuit with resonant frequency ω_{12} is

$$P(f) \sim \frac{1}{1+Q^2\left(\frac{\omega}{\omega_{12}} - \frac{\omega_{12}}{\omega}\right)^2}$$

$$\approx \frac{1}{1+\left(\frac{2Q}{\omega_{12}}\right)^2 \Delta\omega^2}$$

Upon comparison one might define the equivalent Q of a resonance line as

$$Q_{equiv} \equiv \frac{\omega_{12}}{2} T_2$$

at the one-half power points

$$\Delta f = \frac{f_{12}}{Q_{equiv}} = \frac{1}{\pi T_2}$$

or

$$\Delta H = \frac{2\pi}{\gamma} \Delta f = \frac{2}{\gamma T_2}$$

5. Multilevel Rate Equations

Now take the case where there are three levels available, (figure A-4). Some equations analogous to the two level equations can be written

$$n_1 + n_2 + n_3 = N \tag{1}$$

and

$$\begin{aligned}
\frac{dn_1}{dt} &= -(w_{12} + w_{13})n_1 + w_{21}n_2 + w_{31}n_3 \\
\frac{dn_2}{dt} &= w_{12}n_1 - (w_{21} + w_{23})n_2 + w_{32}n_3 \\
\frac{dn_3}{dt} &= w_{13}n_1 + w_{23}n_2 - (w_{31} + w_{32})n_3
\end{aligned} \tag{2}$$

At thermal equilibrium for any two levels i and j where $E_i > E_j$:

$$\frac{N_i}{N_j} = e^{\frac{-(E_i - E_j)}{kT}} = e^{-\frac{hf_{ij}}{kT}} \tag{3}$$

and again the spontaneous transition probabilities

$$\frac{w_{ij}}{w_{ji}} = \frac{N_j}{N_i} \tag{4}$$

A spin-lattice relaxation time can also be defined as

$$w_{ij} = w_{ji} = \frac{1}{2T_{1\,ij}} \tag{5}$$

There is no simple analogy to the Δn equations of the two level system. Furthermore, the $T_{1\,ij}$ defined above is not a true time constant of the system. If perturbed, the population of each level would relax back toward thermal equilibrium creating a series of exponential terms whose time constants would be combinations of the various relaxation times.

When an RF signal is applied near one of the resonance frequencies, the terms that must be added to equation (2) are

$$\begin{aligned}
\frac{dn_i}{dt} &= W_{ij}(n_j - n_i) \\
\frac{dn_j}{dt} &= W_{ji}(n_i - n_j)
\end{aligned} \tag{6}$$

and generally $W_{ji} = W_{ij}$

The induced transition probabilities can usually be written [1]

$$W_{ij} = \frac{1}{16}(\gamma H_{ij})^2 g_{ij}(f) \langle \mu_{ij} \rangle^2 \rho^2(\psi_1, \psi_2, \psi_3) \tag{7}$$

where $g_{ij}(f) = \dfrac{2T_{2ij}}{1+(T_{2ij})^2(\omega - \omega_{ij})^2}$

Some additional information on these terms might be helpful. $g_{ij}(f)$ has the form shown if the line shape is ideal and any broadening is due to coupling between individual spins. In most cases however, the resonance lines are broadened by effects such as impurities in the crystal, flaws, strains, and an inhomogeneous DC magnetic field. $\langle \mu_{ij} \rangle^2$ is a measure of the strength of the transition probability between levels i and j, and is zero for a forbidden transition. This matrix element is obtained from a quantum mechanical calculation involving the spin Hamiltonian[2]. In this manner one can find the strong transitions in the paramagnetic material.

Since the magnetic moment matrix element is normalized at the optimum orientation of the RF field, the ρ^2 term compensates for any other orientation. ψ_1, ψ_2, ψ_3 are the direction cosines of H_{ij}. At optimum orientation, $\rho^2(\psi_1, \psi_2, \psi_3)$ is unity and for some other direction, usually perpendicular, it is zero. At a third mutually perpendicular direction ρ^2 will have a maximum, < 1, with respect to angular variations.

1. See also Schulz - DuBois, E. O. Paramagnetic Spectra of Substituted Sapphire - Part I Ruby BSTJ 38 271 (1959).
2. See Appendix B.

6. Power Absorption and Saturation

When a spin relaxes from one level to another, it exchanges one phonon of energy with the vibrating crystal lattice or with another spin. If there is an applied microwave field present at the correct frequency the spin may exchange a photon of electromagnetic energy with the field. In a two level system the rate of downward transitions is $W_{12}\, n_2$ and the rate of upward transitions is $W_{12}\, n_1$. The net power absorbed from the RF field is

$$P_{abs} = W_{12}\,(n_1 - n_2)\, hf_{12} \tag{1}$$

For a very small signal that does not appreciably disturb the thermal equilibrium distribution

$$\Delta n = n_1 - n_2 = \Delta N = \frac{N}{2}\,\frac{hf_{12}}{kT} \tag{2}$$

and the power absorbed becomes

$$P_{abs} = W_{12}\,\frac{N}{2}\left(\frac{hf_{12}}{kT}\right)^2$$

W_{12} is proportional to H_{12}^2 which is in turn proportional to the applied RF power. Thus, for very small signals, the power absorbed will vary linearly with applied power.

However, when the applied power is increased, the transitions induced will become far greater than the thermal relaxation process upon which the analysis above is based. Therefore, one can go to an expression for Δn developed from equation (A. 2-9) and equation (A. 3-1).

$$\frac{d\Delta n}{dt} = -\left(\frac{\Delta n - \Delta N}{T_1}\right) - 2W_{12}\,\Delta n \tag{3}$$

When the system reaches equilibrium with the signal applied

$$\frac{d\Delta m}{dt} = 0$$

$$\Delta m = \frac{\Delta N}{1 + 2W_{12}T_1} \tag{4}$$

If the applied signal is at f_{12} and is oriented properly

$$\Delta m = \frac{\Delta N}{1 + \left(\frac{\gamma H_{12}}{2}\right)^2 T_1 T_2} \tag{5}$$

For a large signal the Δm will become very small. This fact is very important in pumping a solid state maser.

Combining equations (1) and (4)

$$P_{abs} = \Delta N h f_{12} \frac{W_{12}}{1 + 2T_1 W_{12}}$$

at resonance this becomes

$$P_{abs} = \frac{N}{16} \frac{(hf_{12})^2}{kT} T_2 \frac{(\gamma H_{12})^2}{1 + \frac{T_1 T_2}{4}(\gamma H_{12})^2}$$

which has a limiting value of

$$P_{abs} = \frac{N}{4} \frac{(hf_{12})^2}{kTT_1}$$

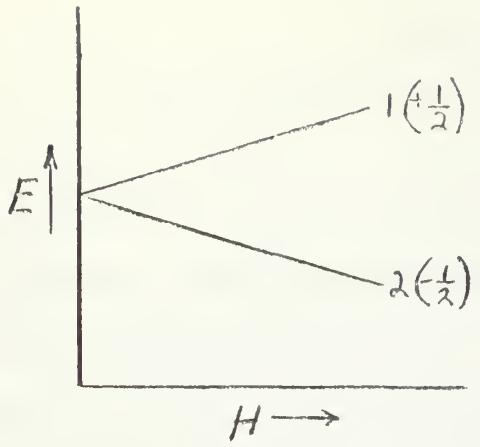

Figure A-1

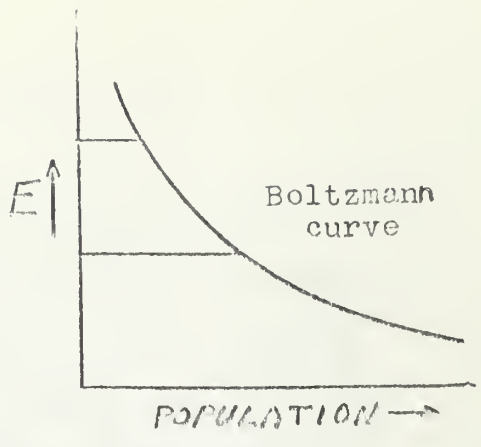

Figure A-2

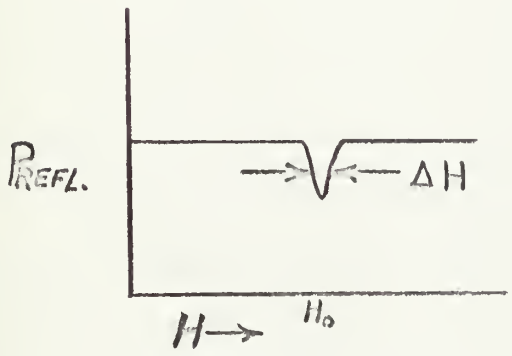

Figure A-3(a)

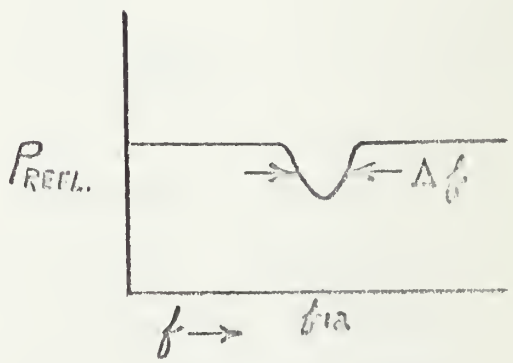

Figure A-3(b)

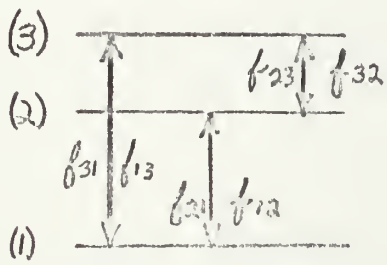

Energy levels

Figure A-4

APPENDIX B

Spin Hamiltonian of Rutile Doped with Fe^{+++}[1]

The Fe^{+++} in rutile has two possible sites per unit cell. The axes used for the spin Hamiltonian are such that Z for site I is in the [110] direction and Z' for site II is in the [$\bar{1}$10] direction. Y and Y' are both parallel to [001].

$$\mathcal{H} = g\beta \underline{H} \cdot \underline{S} + D\left(S_z^2 - \frac{35}{12}\right) + E\left(S_x^2 - S_y^2\right) + \frac{a}{6}\left(S_x + S_y + S_z - \frac{707}{16}\right) + \frac{Z}{36} F\left(S_z^4 - \frac{95}{14} S_z^2 + \frac{81}{16}\right)$$

D = 20.35 ± .1	kmc/sec	g = 2.000 ± .005	
E = 2.21 ± .07	"	S = 5/2	
$\underline{a}$ = 1.1 ± .2	"	H in kilogauss	
F = .5 ± .3	"		

This agrees to within 1% with experimental data. The zero field splittings are 43.3-.1kmc/sec and 81.3-kmc/sec. Relaxation times of 4×10^{-3} sec and $.1 \times 10^{-3}$ sec at X band with T = 1.4°K and T = 78°K respectively have been measured. The frequency variation of T_1 appears to be $\propto \frac{1}{f^2}$.

Figure B-1 is a diagram of the rutile structure.

1. Letter from David L. Carter of Columbia University to Roy W. Roberts of Melabs. A more complete article containing this information is to be published in The Physical Review.

Note: A preprint of Mr. Carter's article was received shortly before this paper was printed.

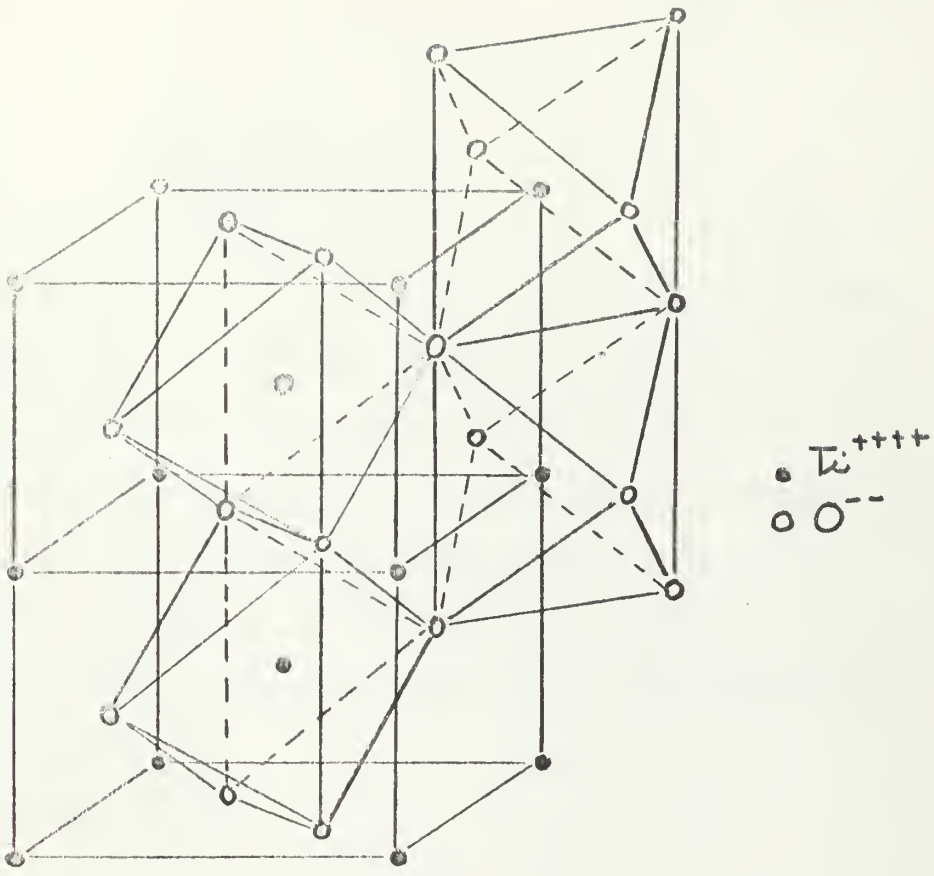

Crystal structure of rutile [13]

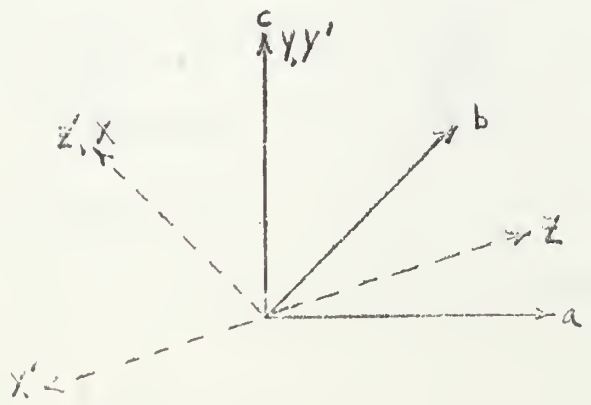

Hamiltonian axes

Figure B-1

APPENDIX C

Noise Figure and Noise Temperature [2]

The noise figure (F) of an amplifier, or any other network for that matter, is defined as the power ratio:

$$F = \frac{\left(\frac{\text{Signal}}{\text{Noise}}\right)_{\text{input}}}{\left(\frac{\text{Signal}}{\text{Noise}}\right)_{\text{output}}} \tag{1}$$

Since no device that is presently known is capable of reducing the noise level at its input terminals without also reducing the signal level, the smallest value of F is one, or zero db. The effective noise input power of equation (1) is, by definition; equivalent to the Johnson noise power per cycle which would be generated by a resistor at the input terminals equivalent to the input resistance of the device. This theoretical ambient noise power per cycle is:

$$N_0 = kT_0$$

where k = Boltzmann's constant

$$T_0 = 290^\circ K$$

If P_n is defined as the "effective noise power" at the input terminals of a device with a gain of G:

$$F = \frac{\frac{S}{kT_0}}{\frac{GS}{GkT_0 + GP_n}} = 1 + \frac{P_n}{kT_0} \tag{2}$$

$$P_n = kT_0(F-1) \tag{3}$$

By defining another quantity, Te, as the "effective input noise temperature"

$$P_n = kT_e \tag{4}$$

or $$T_e = T_0 (F-1) \tag{5}$$

Therefore, if the noise figure of a network is unity, its effective noise temperature is 0°K.

The effect of cascading two networks is shown by

$$F_2 = \frac{\frac{G_1 S}{G_1 k T_0 + G_1 P_{n1}}}{\frac{G_2 G_1 S}{G_2 (G_1 k T_0 + G_1 P_{n1}) + G_2 P_{n2}}} \tag{6}$$

or
$$F_1 F_2 = F_{12} = F_1 + \frac{(F_2 - 1)}{G_1} \tag{7}$$

$$(F_{12} - 1) T_0 = (F_1 - 1) T_0 + \frac{(F_2 - 1)}{G_1} T_0$$

This equation can be readily converted to:

$$T_{e12} = T_{e1} + \frac{T_{e2}}{G_1} \tag{8}$$

Equation (8) shows that the overall noise temperature of two cascaded networks is minimized by a first stage of high gain and low noise temperature. If three networks are cascaded the noise temperature of the combination is:

$$T_{e123} = T_{e1} + \frac{T_{e2}}{G_1} + \frac{T_{e3}}{G_1 G_2}$$

Here it is even more apparent that the noise temperature of the combination approaches the noise temperature of the first stage.

From equation (5) one can show that

$$F = 1 + \frac{T_e}{290}$$

For a maser, T_e is generally on the order of 5-10°K. Therefore, it is unwieldy to speak of F in decibels (.074 db for 5°K) so noise temperature is normally used when referring to a maser system.

Additionally, it might be noted that cascading an amplifier of noise figure F with a transmission line of loss L results in an effective noise temperature of (FL-1) T_o for the combination.